

# Synthesis of $\text{TiO}_2$ and $\text{MgAl}_2\text{O}_4$ Nano Composites for the Enhancement of Antibacterial Applications

K. S. Bhargavi and Anindita Bose\*

Department of Physics, Presidency University, Bangalore – 560064, Kanataka, India;  
[anindita@presidencyuniversity.in](mailto:anindita@presidencyuniversity.in)

## Abstract

In this study, nano composites of titanium dioxide and magnesium aluminate samples were synthesized using the chemical sol-gel method. Investigations are conducted on the antibacterial behavior of a low concentration of transition metal oxides like  $\text{TiO}_2$ , with pre-transition metal oxides, such as  $\text{MgO}$  and  $\text{Al}_2\text{O}_3$ . The goal of the current work is to apply various nano composite samples of  $(\text{TiO}_2)_x$  and  $\text{MgAl}_2\text{O}_4$  with 4 and 10 wt% of  $\text{TiO}_2$  in  $\text{MgAl}_2\text{O}_4$  respectively, for antibacterial applications. The composite samples were examined using Scanning Electron Microscopy (SEM), Fourier Transform Infrared Spectroscopy (FTIR), and the X-ray diffraction pattern. Gramme - positive bacteria *S. aureus* and *B. subtilis*, as well as gramme-negative bacteria *P. aeruginosa* and *S. typhimurium*, were tested for in the samples' antibacterial behaviour.

**Keywords:** Antibacterial Activity, Gram Positive and Negative Bacteria, Metal Oxides, Sol-Gel Method

## 1.0 Introduction

Over the past ten years, nano science and technology have become the cutting edge of science and technology. The industrial revolution is significantly influenced by nanotechnology. Interest in studying the toxicity and antibacterial properties of metal oxide nanomaterials has increased recently<sup>1</sup>. Understanding the toxicity mechanisms of these materials is essential in order to predict their ecotoxicity and environmental impact because they are used in a variety of consumer products as well as antimicrobial agents<sup>2</sup> and cancer treatment agents<sup>3</sup>. An expanding global concern is the problem faced by bacterial resistance. So it is necessary to fabricate more potential antibacterial agents to control the bacterial growth<sup>4</sup>. The morphology, composition, size, crystallinity, shape of a nano particle plays a significant role in determining its intrinsic properties. To achieve a uniform material response, a narrow size distribution

is provided by nano-scale particles<sup>5</sup>. Because they are stable under difficult processing circumstances and are generally viewed as safe materials for both people and animals, calcium oxide, zinc oxide, titanium dioxide, and magnesium oxide are particularly intriguing metal oxides<sup>6</sup>. Magnesium oxide is an intriguing basic oxide that is used in the synthesis of refractory ceramics, adsorption, and catalysis<sup>7</sup>. It is a special solid with a high ionic character, a simple crystal structure, and the ability to be prepared in a variety of ways with different particle sizes and shapes<sup>8</sup>. The large concentration of edge sites and structural flaws on the surface of nano crystalline magnesium oxide particles have been reported to give them a high specific surface and reactivity<sup>9</sup>. Magnesium aluminate, also known as  $\text{MgAl}_2\text{O}_4$  is a familiar spinal material using in a variety of applications, including those for (i) fusion reactor structural materials, (ii) catalyst or catalyst support, (iii) microwave dielectric and ceramic capacitors, (iv) humidity sensors, and (v) microwave

\*Author for correspondence

dielectric materials<sup>10</sup>. Additionally, Magnesium aluminate has good chemical resistance, a low density (3.58 g/cm<sup>3</sup>), a high melting point (2135 °C), and excellent strength at very high temperatures<sup>11</sup>. The preparation techniques play a significant role in the synthesis of MgAl<sub>2</sub>O<sub>4</sub> with specific properties like uniform size distribution, low particle size, high purity and chemical homogeneity<sup>12</sup>. A versatile metal oxide with special technological characteristics, Titanium Dioxide (TiO<sub>2</sub>) is used in photo catalysts, solar cells, sensors, memory devices, and bactericidal products. The crystal structure of TiO<sub>2</sub> is related to its antibacterial properties<sup>13</sup>. It is believed that the production of Reactive Oxygen Species (ROS), which occurs during oxidative stress, is an especially significant mechanism for TiO<sub>2</sub> nano particles. ROS then damage DNA at a specific site<sup>14</sup>. For the dielectric and gas sensing studies, MgAl<sub>2</sub>O<sub>4</sub> with low concentrations of TiO<sub>2</sub> is used more successfully<sup>15</sup>. The preparation of nano composites of titanium dioxide and magnesium aluminate samples using synthesis techniques like sol-gel is the focus of this study. At a calcination temperature of 973K, the effects of TiO<sub>2</sub> addition on the microstructures of MgAl<sub>2</sub>O<sub>4</sub> nano particles are being studied.

## 2.0 Experimental Procedure

### 2.1 Synthesis of Magnesium Oxide

Magnesium nitrate was also used as a raw material for the manufacture of magnesium oxide nanoparticles in addition to sodium hydroxide. For the standard experimental procedure, 0.2M magnesium nitrate was dissolved in 100ml of distilled water, and 0.5M sodium hydroxide solution was gradually added while stirring to the prepared magnesium nitrate solution. A white precipitate of magnesium hydroxide eventually became apparent in the beaker. The stirring went on for another 30 minutes. The pH of the solution was maintained at 12.5. The precipitate was filtered, cleaned with methanol three to four times, centrifuged for five minutes at 5000 rpm, dried at room temperature, and finally purified to remove ionic impurities. The dried samples underwent two hours of annealing at 573K

### 2.2 Synthesis of Magnesium Aluminate (MA)

Chemical Sol-gel method was used to prepare the

MgAl<sub>2</sub>O<sub>4</sub> samples. Double-distilled water was stirred with MgO, Aluminum oxide, and PEG to create a consistent mixture. The prepared mixture was slowly added to ethanol and stirred for eight hours to get magnesium aluminium hydroxide. For the purpose of fabricating magnesium aluminate samples, the obtained mixture solution was dried at 973K for 4 hours.

### 2.3 MgAl<sub>2</sub>O<sub>4</sub> Nano Composite with TiO<sub>2</sub> Synthesis (MAT)

The prepared MgAl<sub>2</sub>O<sub>4</sub> mixture is mixed with a small amount of TiO<sub>2</sub> (by 4 and 10 weight percentage of TiO<sub>2</sub>) to form TiO<sub>2</sub> and MgAl<sub>2</sub>O<sub>4</sub> composites. The final mixture was stirred for six hours at 473 K in a magnetic stirrer. The calcined mixture was dried in a hot air oven for ten hours at 673 K. The samples are all given eight hours to cool at room temperature.

### 2.4 Antibacterial Procedure

Bacterial test cultures were purchased from Chandigarh's Institute of Microbial Technology's Microbial Type Culture Collection (MTCC). Cultures of the Gram-positive bacteria *S. aureus* and *B. subtilis*, as well as the Gram-negative bacteria *P. aeruginosa* and *S. typhi*, were cultivated on nutrient agar media utilised for the antibacterial activity experiment.

The antibacterial activity of chemical substances was evaluated using the dual-culture agar diffusion assay Under aseptic circumstances, 20 ml of sterilised Nutrient agar media was added to petridishes and left to set. 100 µl of standardized test microbial inoculums of the Gram-positive bacteria *S. aureus*, *B. subtilis*, and the Gram-negative bacteria *P. aeruginosa* and *S. typhi* were spread evenly using glass loop after the media had solidified. The sample was diluted with DMSO to a concentration of 1mg/ml before being added to plates to test for antibacterial compound diffusion. After that, the plates were incubated for 24 hours at 37°C. The diameter of the inhibition zone surrounding the well was measured in millimetres (mm), and the average of three different agar discs was taken to evaluate the extent of the antibacterial activity. It was thought that chloramphenicol was standard practice.

## 3. Results and Discussion

### 3.1 Structural Analysis

Figure 1 displays the acquired SEM images for each sample. The homogeneous spherical particles in the sample MA have an irregular shape and a dispersed morphology. The MAT-4, MAT-10 sample particles are exhibiting a porous nature. Isomorphous grains of MgAl<sub>2</sub>O<sub>4</sub> are visible in the observed SEM image, suggesting potential differences in particle structure.

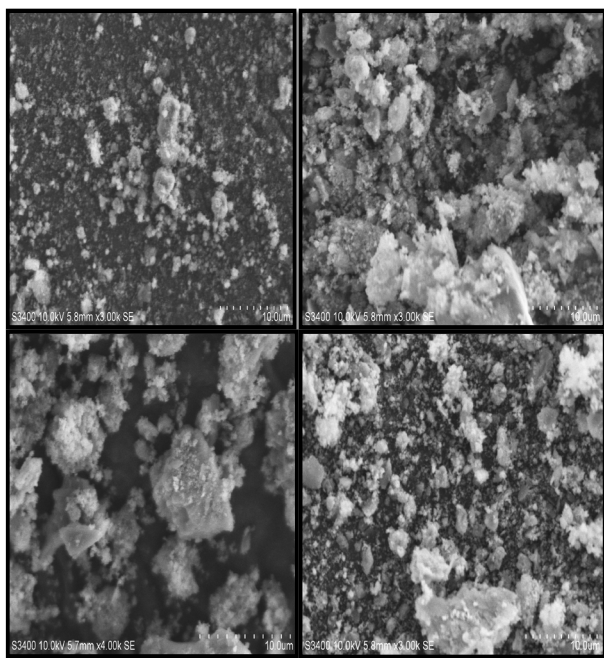


**Figure 1.** SEM images of the samples MA, MAT-4 and MAT-10.

### 3.2 Morphological Analysis

Figure 2 displays the XRD patterns of the samples MA, MAT-4, and MAT-10. At diffraction angle  $2\theta = 29.39$ ,  $30.93$ ,  $36.81$ ,  $42.80$ ,  $51$ , and  $62.12$ , the crystalline phase

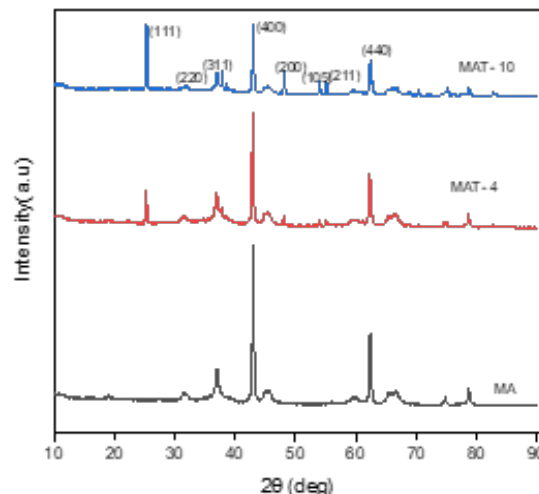


**Figure 2.** XRD peaks of the samples MA, MAT-4, and MAT-10.

of MgAl<sub>2</sub>O<sub>4</sub> displays well-defined and intense main peaks with planes (111), (220), (311), (400), (211), and (440) that match the standard data connected with the JCPDS file no. 21152. (cubical crystal structure with face centered lattice)<sup>16</sup>. XRD spectra confirming the formation of MgAl<sub>2</sub>O<sub>4</sub> and TiO<sub>2</sub> composites.

Scherer's equation was used to determine the samples' average crystalline sizes, which are shown in Table 1. 31.14nm, 30.86nm, and 24.78nm are the average crystalline size of the samples, MA, MAT-4, and MAT-10 respectively.

### 3.3 FTIR Analysis

As shown in Figure 3, the functional groups of the samples are examined using FT-IR in the absorption range 4000-400 cm<sup>-1</sup>. The hydroxyl (-OH) groups from Mg(OH)<sub>2</sub> and the stretching vibrations of adsorbed water molecules are responsible for the peak measured at 3521cm<sup>-1</sup><sup>17</sup>. The bending mode of the H-O-H bond is responsible for the absorption band seen at 1590.5 cm<sup>-1</sup>. For samples MA,

**Table 1.** Crystallite size and EDAX composition of the prepared samples

Sample name	Crystallite size (XRD)	EDAX composition of elements			
		Mg	Al	Ti	O
MA	31.14nm	33.96	14.75	-	51.29
MAT-4	30.86nm	25.80	18.38	3.10	52.73
MAT-10	24.78nm	26.86	13.25	8.54	51.35

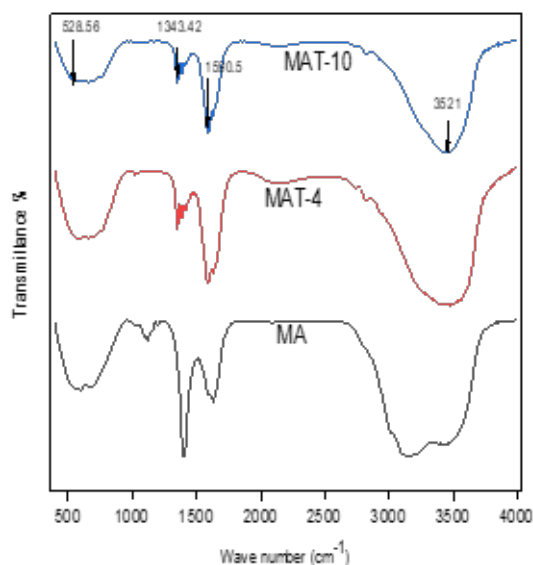


**Figure 3.** FTIR spectra of samples MA, MAT-4 and MAT-10.

MAT-4, and MAT-10, the two bands seen at 800 and 528.56  $\text{cm}^{-1}$  are due to the  $\text{AlO}_6$  group and the stretching of the  $\text{MgO}_4$  lattice brought on by the formation of  $\text{MgAl}_2\text{O}_4$  spinel's.

The weak bands seen at 800-400  $\text{cm}^{-1}$  suggest that samples MA and MAT-4 have a slightly brittle crystalline structure. The  $\text{CH}_2$  group of PEG accounts for the broad peak seen at roughly 1400  $\text{cm}^{-1}$  (bending-scissoring vibration). The Ti-O-Ti stretching modes of the  $\text{TiO}_2$  anatase phase are what cause the 800 - 450  $\text{cm}^{-1}$  vibration peak that was observed. The composition of  $\text{MgO}$  changes very little in the end<sup>18</sup>.

### 3.4 Antibacterial Assay

The antibacterial properties of pure  $\text{MgAl}_2\text{O}_4$  and  $\text{MgAl}_2\text{O}_4$  doped with  $\text{TiO}_2$  were evaluated against the gram-positive bacteria *S. aureus* and *B. subtilis* as well as the gram-negative bacteria *P. aeruginosa* and *S. typhi* using the well diffusion assay.  $\text{TiO}_2$  doped  $\text{MgAl}_2\text{O}_4$  was examined at two different concentrations, 4% and 10%. The bactericidal properties of  $\text{TiO}_2$  doped  $\text{MgAl}_2\text{O}_4$  and pure  $\text{MgAl}_2\text{O}_4$  differ noticeably. Figure 4 shows clearly that bacterial colonies have grown up around the disc that is filled with  $\text{TiO}_2$ -doped  $\text{MgAl}_2\text{O}_4$ <sup>19</sup>. However, it was observed that these bacterial colonies were significantly reduced and a clear zone of inhibition formed surrounding discs loaded with  $\text{TiO}_2$  doped  $\text{MgAl}_2\text{O}_4$ . The formation of an inhibitory zone has demonstrated the antibacterial efficacy of  $\text{MgAl}_2\text{O}_4$  doped with  $\text{TiO}_2$ . In comparison to pure  $\text{MgAl}_2\text{O}_4$ , adding  $\text{TiO}_2$  at increasing concentrations resulted in excellent antibacterial efficacy. Because different concentrations of  $\text{TiO}_2$  were used for doping,  $\text{MgAl}_2\text{O}_4$  showed a variation in antibacterial performance. These results suggest that increasing the  $\text{TiO}_2$  concentration in  $\text{MgAl}_2\text{O}_4$  significantly increases the antibacterial activity of nanoparticles.  $\text{TiO}_2$  ions from the doped nano material gradually diffused into the seeded agar during incubation<sup>20</sup>. Reactive oxygen species are produced as a result of the attachment of  $\text{TiO}_2$  ions to cell membranes, interactions with protein thiol groups, and inactivation of respiratory enzymes. With the test of all the strains, a significant increase in the diameters of the zones of inhibition with increasing  $\text{TiO}_2$  capping (4% and 10%) in comparison to pure  $\text{MgAl}_2\text{O}_4$  NPs could be seen from Figure 1. Reactive oxygen species, particularly

**Table 2.** Inhibition zone diameter of  $\text{TiO}_2$  doped  $\text{MgAl}_2\text{O}_4$  nano composites against different bacterial pathogens.

SI. No.	Name	<i>P. aeruginosa</i>	<i>B. subtilis</i>	<i>S. aureus</i>	<i>S. typhi</i>
1	$\text{MgAl}_2\text{O}_4$	7 mm	6 mm	7 mm	7 mm
2	4% $\text{TiO}_2$ $\text{MgAl}_2\text{O}_4$	10mm	9mm	8 mm	9 mm
3	10% $\text{TiO}_2$ $\text{MgAl}_2\text{O}_4$	12 mm	11 mm	12 mm	12 mm

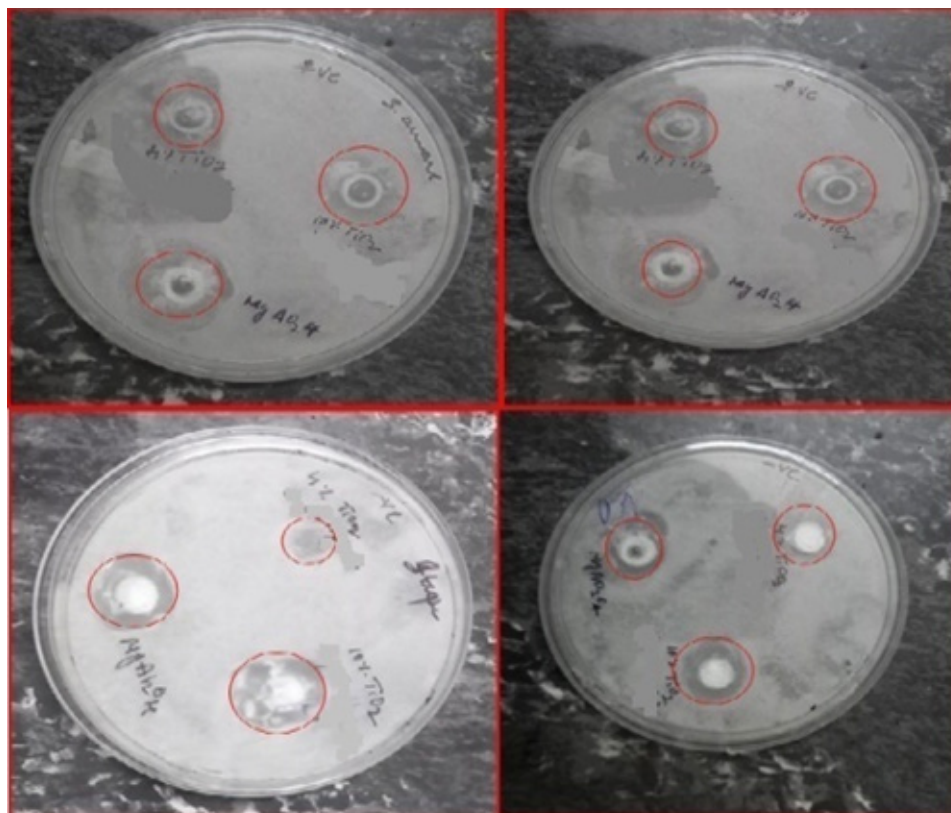


**Figure 4.** Antibacterial activity of 4%, & 10%  $\text{TiO}_2$  and  $\text{MgAl}_2\text{O}_4$  nano composites with zone of inhibition of (a) *Staphylococcus aureus* (b) *S. typhi* (c) *Bacillus subtilis* (d) *Pseudomonas aeruginosa*.

hydroxyl radicals, inhibit bacterial DNA replication and cause the outer membranes to breakdown, which causes phospholipid peroxidation and ultimately cell death<sup>21</sup>.

## 4.0 Conclusion

Sol-gel synthesis of nanocomposites of (4,10 c/o)  $\text{TiO}_2$  and  $\text{MgAl}_2\text{O}_4$  for antibacterial applications is done in this study. The formula developed by Debye Scherer is used to gauge the samples' crystallite sizes.; it was found that the crystallite size decreased as the  $\text{TiO}_2$  concentration increased. The samples of  $\text{MgAl}_2\text{O}_4$  and  $\text{MgAl}_2\text{O}_4$  combined with 4&10 % of  $\text{TiO}_2$ , have crystallite sizes of 31.14, 30.86, and 24.78 nm, respectively. The microbial cells and the nano composites appear to interact directly, changing the shape of the cells significantly and interfering with their regular structure and function. The nano composites clearly Inhibiting cell growth and causing the death of various microorganisms with higher antimicrobial activity against both gram positive *S. aureus*,

*B. subtilis* and gram negative *P. aeruginosa* and *S. typhi* bacteria. Therefore the nano composites of (4,10 %)  $\text{TiO}_2$  and  $\text{MgAl}_2\text{O}_4$  are good for the anti bacterial applications

## 5.0 References

1. Foster HA, Ditta IB, Varghese S, Steele A. Photocatalytic disinfection using titanium dioxide: spectrum and mechanism of antimicrobial activity. *Appl Microbiol Biotechnol.* 2011; 90:1847-1868.
2. Makhluif S, Dror R, Nitzan Y, Abramovich Y, Jelinek R, Gedanken A. Microwave-assisted synthesis of nanocrystalline MgO and its use as a bactericide. *Adv Funct Mater.* 2005; 15(10):1708-1715.
3. Krishnamoorthy K, Moon JY, Hyun HB, Cho SK, Kim S-J. Mechanistic investigation on the toxicity of MgO nanoparticles toward cancer cells. *J Mater Chem.* 2012; 22(47):24610-617.
4. Regiel-Futyra A, Kus-Liškiewicz M, Sebastian V, Irusta S, Arruebo M, Kyzioł A, Stochel G. Development of non-cytotoxic silver-chitosan nanocomposites for efficient

- control of biofilm-forming microbes. *RSC Adv.* 2017; 7(83):52398-413.
5. Dickson RM, Lyon LA. Unidirectional plasmon propagation in metallic nanowires. *J Phys Chem B.* 2000; 104(26):6095-98.
  6. Stoimenov PK, Klinger RL, Marchin GL, Klabunde KJ. Metal oxide nanoparticles as bactericidal agents. *Langmuir.* 2002; 18(17):6679-86.
  7. Xu B-Q, Wei J-M, Wang H-Y, Sun K-Q, Zhu Q-M. Nano-MgO: novel preparation and application as support of Ni catalyst for CO<sub>2</sub> reforming of methane. *Catal Today.* 2001; 68(1-3):217-25.
  8. Morris RM, Klabunde KJ. Formation of paramagnetic adsorbed molecules on thermally activated magnesium and calcium oxides. Characteristics of the active surface sites. *Inorg Chem.* 1983; 22(4):682-7.
  9. Klabunde KJ, Stark J, Koper O, Mohs C, Park D, Decker S, Jiang Y, Lagadic I, Zhang D. Nanocrystals as stoichiometric reagents with unique surface chemistry. *J Phys Chem.* 1996; 100(30):12142-53.
  10. Iqbal MJ, Ismail B, Rentenberger C, Ipser H. Modification of the physical properties of semiconducting MgAl<sub>2</sub>O<sub>4</sub> by doping with a binary mixture of Co and Zn ions. *Mater Res Bull.* 2011; 46(12):2271-7.
  11. Ismail B, Hussain ST, Akram S. Adsorption of methylene blue onto spinel magnesium aluminate nanoparticles: adsorption isotherms, kinetic and thermodynamic studies. *Chem Eng J.* 2013; 219:395-402.
  12. Shiono T, Shiono K, Miyamoto K, Pezzotti G. Synthesis and characterization of MgAl<sub>2</sub>O<sub>4</sub> spinel precursor from a heterogeneous alkoxide solution containing fine MgO powder. *J Am Ceram Soc.* 2000; 83(1):235-7.
  13. Haghghi F, Roudbar Mohammadi S, Mohammadi P, Hosseinkhani S, Shipour R. Antifungal activity of TiO<sub>2</sub> nanoparticles and EDTA on *Candida albicans* biofilms. *Infect Epidemiol Microbiol.* 2013; 1(1):33-8.
  14. Roy AS, Parveen A, Koppalkar AR, Prasad MA. Effect of nano-titanium dioxide with different antibiotics against methicillin-resistant *Staphylococcus aureus*. *J Biomater Nanobiotechnol.* 2010; 1(1):37.
  15. Surendran K, Mohanan P, Sebastian M. The effect of glass additives on the microwave dielectric properties of Ba (Mg<sub>1/3</sub>Ta<sub>2/3</sub>) O<sub>3</sub> ceramics. *J Solid State Chem.* 2004; 177(11): 4031-46.
  16. Kurien S, Sebastian S, Mathew J, George K. Structural and electrical properties of nano-sized magnesium aluminate. 2004.
  17. Ping LR, Azad AM, Dung TW. Magnesium aluminate (MgAl<sub>2</sub>O<sub>4</sub>) spinel produced via self-heat-sustained (SHS) technique. *Mater Res Bull.* 2001; 36(7-8):1417-30.
  18. Rufner J, Anderson D, van Benthem K, Castro RH. Synthesis and sintering behavior of ultrafine (<10 nm) magnesium aluminate spinel nanoparticles. *J Am Ceram Soc.* 2013; 96(7):2077-85.
  19. Matsumura Y, Yoshikata K, Kunisaki S-i, Tsuchido T. Mode of bactericidal action of silver zeolite and its comparison with that of silver nitrate. *Appl Environ Microbiol.* 2003; 69(7):4278-81.
  20. Bahadur J, Agrawal S, Panwar V, Parveen A, Pal K. Antibacterial properties of silver-doped TiO<sub>2</sub> nanoparticles synthesized via sol-gel technique. *Macromol Res.* 2016; 24(6):488-93.
  21. Guo B, et al. Sol gel derived photocatalytic porous TiO<sub>2</sub> thin films. *Surf Coatings Technol.* 2005; 198(1-3):24-9.